

# Design, Synthesis, Cytotoxic Evaluation and Docking Study of Dihydrobenzofuran Derivatives as a Potential Candidate for Cancer Therapy

Akeel Abo Alard\*<sup>1</sup>

<sup>1</sup>Department of Pharmaceutical Chemistry, Faculty of Pharmacy, University of Kufa, Najaf, Iraq

\*Corresponding Author: Akeel Abo Alard: akeela.aboalard@uokufa.edu.iq

**Abstract**—Overexpression of CAIX for many research represent as an attractive therapeutic target in oncology. Therefore, a number of novel dihydrobenzofuran derivatives (5a–5d) was designed, synthesised, and anticancer activity was investigated using both molecular docking simulations and cytotoxicity testing. The synthetic route applied some of key reagents such as sulfanilamide, thiourea and substituted dihydrobenzofuran. For computational docking analyses Schrodinger Maestro software release 2021-1 was used for this purpose. While, cell viability was evaluated via the MTT assay with using doxorubicin as a control compound. The newly prepared derivatives exhibited inhibitory effects on cancer cell survival. All compounds 5a-d achieved promising docking S-scores, suggesting stronger interactions within the receptor's active site. Structural features such as chlorine, methyl, methoxy substituent and the dihydrobenzofuran moiety may enhance molecular flexibility and receptor engagement. In addition, structural incorporation of the thiazole moiety enhanced molecular flexibility and improved receptor-binding affinity. Also, formation of the metal complex further increased the compounds' ability to suppress cellular proliferation. Regard to *in vitro* cytotoxicity study, among the tested compound 5b demonstrated moderate cytotoxic activity versus MCF-7 and HCT116 cell lines with the  $IC_{50}$  values of  $8.68 \pm 0.87$  and  $7.24 \pm 0.81$  respectively. Compound 5d, also exhibited moderate activity versus the MCF-7 with an  $IC_{50}$  value of  $9.24 \pm 0.90 \mu\text{M}$ . However, this derivative exhibited reduced activity versus the HCT116 with an  $IC_{50}$  value of  $15.33 \pm 1.21 \mu\text{M}$ . Moreover, both 5a and 5c demonstrated a low level of cytotoxic activity effect on cell lines. These results suggest that the dihydrobenzofuran scaffold provides a promising foundation for further optimisation in anticancer drug development.

**Keywords**— Carbonic anhydrase; sulfonamide, docking study; dihydrobenzofuran, cytotoxicity.

## I. INTRODUCTION

Generally, cancer represent one of the most formidable global health challenges, accounting for a substantial proportion of premature mortality and limiting gains in life expectancy worldwide [1]. Data collected from the WHO revealed that cancer is one of the main causes leading to death before the age of 70 in the majority of countries [2]. In this context, breast cancer has an extra challenge: some types of it gradually become resistant to treatment, which makes therapies less effective and allows the disease to keep progressing. Overcoming treatment resistance is a major challenge in cancer treatment and is therefore a key research priority [3]. Targeting the tumour microenvironment (TME) to overcome resistance to the available chemotherapy is understudied. carbonic anhydrases (CAs) is one component of the TME that have received considerable attention [4]. These are zinc-dependent enzymes that are expressed in various species and are encoded by several related genes [5].

CAs catalyse a reversible reaction that converts carbon dioxide ( $\text{CO}_2$ ) into bicarbonate ( $\text{HCO}_3^-$ ) and a proton. This reaction has an important role in maintaining pH balance and supporting many physiological processes. In humans, 15  $\alpha$ -carbonic anhydrase isoforms have been identified, 12 of which are catalytically active. These isoforms differ in their expression, intracellular localization, and enzymatic activity across different tissues [6]. Under hypoxic (low oxygen) conditions, hypoxia-inducible factor-1 (HIF-1) induces the expression certain CA isoforms, particularly CAIX and

CAXII. CAIX, in particular, is expressed at very low levels in normal tissues but is significantly upregulated in different types of cancer. Together with enhanced anaerobic glycolysis, these enzymes contribute to acidifying the TME, which in turn supports cancer cell survival, invasion, and proliferation. Because of their cancer-associated expression, they represent potential therapeutic targets to improve selectivity and reduce side effects of chemotherapy [7–9].

Most classical carbonic anhydrase inhibitors (CAIs) interact with the zinc ion ( $\text{Zn}^{2+}$ ) located in the enzyme's active site, where the coordination geometry shifts between tetrahedral and trigonal bipyramidal forms during inhibition [10]. Sulfonamides are one of the most common classes of CAIs and interact with this zinc centre. Advances in understanding the structure of the active site have enabled more rational drug design, with aryl-sulfonamides showing particularly strong binding affinity [11]. However, achieving selectivity between different isoforms is still challenging. One approach, known as the “tail approach,” involves modifying substituents on the aromatic ring of the sulfonamide, which is associated with improving isoform selectivity [12].

Thiazole is another important structural motif in medicinal chemistry. It is a heteroaromatic ring containing both nitrogen and sulfur atoms and is commonly found in many bioactive compounds [13]. Its electronic properties and the reactive hydrogen at the C-2 position make it suitable for a variety of chemical transformations. Thiazole-containing compounds have already been investigated in oncology, both in preclinical and clinical settings. This suggests their relevance in

anticancer drug development [14–16]. Furthermore, metal complexes derived from sulfonamide-based CAIs have been found to exhibit enhanced inhibitory activity compared to their parent compounds [17]. This increased activity results from the following mechanism: the sulfonamide group coordinates with the zinc ion, while the metal centre may interfere with proton transfer within the enzyme. In addition, controlled dissociation of these complexes allows effective inhibition at relatively low concentrations [18–21].

Therefore, this study aims to design and synthesise new hybrid molecules that combine a sulfonamide group, acting as a carbonic anhydrase inhibitor, with a dihydrobenzofuran scaffold. Corresponding silver complexes were also prepared, and their cytotoxic activity was assessed using both computational and experimental approaches. This combined approach aims to exploit structural synergy to improve anticancer activity while targeting CA-associated tumour biology.

## II. MATERIALS AND METHODS

### Chemistry of synthesised dihydrobenzofuran moieties analogues

All chemicals materials and pure solvents used in this study were supplied from commercial sources, including Meerck, abor, Aldrich, Theemo Fisher and Thoomas Bakerr. Reaction progress, the synthesised compounds purity, were assessed using ascending thin-layer chromatography (TLC), with appropriate solvent mixture employed as the mobile phase. All analogues structurally characterised by Proton (1H) and carbon-13 (13C) nuclear magnetic resonance spectra. NMR spectra were obtained using Bruker instrumentation at 400 MHz (1H) and 100 MHz (13C) with DMSO- $d_6$  used as a solvent.

#### Chemical Synthesis:

##### 2-Chloroe-N-(4-sulfamoylphenyl)acetamide (2)[22]

The preparation of compound 2 was made by dissolving sulphaniamide (1g, 5.8 mmol) in THF (20 mL) and then  $K_2CO_3$  (1.6 g, 11.6 mmol) added with continuously stirred on an ice bath. To this mixture drops of chloro-acetyl chloride (0.54 ml, 6.9 mmol in 5 mL THF) was added. Then, continuous stirred to the mixture for 30 min in ice bath and then left for further 3 hours at rt. TLC was used to follow the reaction progress and upon end of reaction, water (40 mL) was added and then extracted with EtOAc. The collected organic layer was then washed with brine and dried over anhydrous  $MgSO_4$ , then solvent evaporation to yielded white solid (88%). Mp = 210–212 °C.  $^1H$  NMR (DMSO- $d_6$ )  $\delta$ : 10.63 (s, 1H, NHCO), 7.86 – 7.79 (m, 4H, Ar-H), 7.28 (s, 2H,  $NH_2SO_2$ ), 4.33 (s, 2H,  $CH_2$ ), TLC:  $R_f$ 0.65<sup>a</sup>.

##### 4-((2-aminothiazol-4-yl) amino) benzene-sulfonamide (3)

Compound 2 (0.4 g, 1.5 mmol) was dissolved in ethanol (40 mL) and then thiourea (0.11 g, 1.5 mmol) was added and left under the refluxed for 10 h. Then, TLC was used to checked the reaction process and upon finishing poured the mixture into ice cold water and the formed ppt was then filtered and washed several times with  $NaHCO_3$  solution. Recrystallisation from absolute ethanol was applied to clean

the crude product. Desired compound obtained as a light beige solid (79%). mp = 107–109 °C,  $^1H$  NMR (DMSO- $d_6$ )  $\delta$ : 8.47 (br, s, 2H, NH<sub>2</sub>), 7.81 (d, 2H, Ar-H), 7.44 (br, s, 1H, NH), 6.98 (s, 2H,  $NH_2SO_2$ ), 6.68 (d, 2H, Ar-H), 5.89 (s, 1H, s, thiazole CH), TLC:  $R_f$ 0.77<sup>a</sup>.

#### Preparation of dihydrobenzofuran derivatives 5a-d: General procedure

For the mixture solution of selected dihydrobenzofuran molecule (2 mmol) dissolved in 40 mL ethanol, two drops of glacial acetic acid and compound 3 was added (0.45 g, 2 mmol). Then, mixture subjected to refluxes for 18 h. The solvent was evaporated and EtAc was added, the resulting organic layers washed with saturated Sod. Bicarbonate solution, and then with NaCl solution sequentially. The collected organic layers dried by using  $MgSO_4$  and filtered. The ppt was then purified through recrystallisation by ethanol to afford the desired analogues (5a–d). Melting points and spectral data for each target derivative are provided in the synthesis section below [23].

##### (Z)-4-((2-(benzofuran-3(2H)-ylideneamino)thiazol-4-yl)amino)benzenesulfonamide (5a)

Follow up the general method above, compound 3 (0.54 g, 2 mmol), two drops of glacial acetic acid and benzofuran-3(2H)-one (0.26 gm, 2 mmol). The final analogue obtained as orange powder (65%). mp = 197–199 °C;  $^1H$  NMR (DMSO- $d_6$ )  $\delta$ : 7.83-7.71 (m, 4H, Aromatic-H), 7.54 (broad s, 1H, N-H), 7.25-7.12 (m, 2H, Ar-H) 6.99 (s, 2H,  $NH_2SO_2$ ), 6.78 (d, 2H, Ar-H), 5.92 (s, 1H, s, thiazole CH), 4.76 (s, 2H, cyclic O-CH<sub>2</sub>).  $^{13}C$  NMR (DMSO- $d_6$ ,  $\delta$ )  $\delta$  198.91, 159.21, 157.86, 105.32, 139.98-74.77 (13 Ar-C), TLC:  $R_f$ 0.78<sup>a</sup>.

##### (Z)-4-((2-((6-chlorobenzofuran-3(2H)-ylidene)amino)thiazol-4-yl)amino)benzenesulfonamide (5b)

Follow up the general method above, compound 3 (0.54 g, 2 mmol), two drops of glacial acetic acid and 6-chlorobenzofuran-3(2H)-one (0.34 gm, 2 mmol). The final analogue obtained as orange powder (65%). mp = 212–215 °C;  $^1H$  NMR (DMSO- $d_6$ )  $\delta$ : 7.88-7.75 (m, 4H, Aromatic-H), 7.51 (broad s, 1H, N-H), 7.22-7.18 (m, 2H, Ar-H) 7.01 (s, 2H,  $NH_2SO_2$ ), 6.56 (d, 1H, Ar-H), 5.97 (s, 1H, s, thiazole CH), 4.66 (s, 2H, cyclic O-CH<sub>2</sub>).  $^{13}C$  NMR (DMSO- $d_6$ ,  $\delta$ ):  $\delta$  196.83, 158.77, 157.69, 104.35, 138.86-73.45 (12 Ar-C), TLC:  $R_f$ 0.74<sup>a</sup>.

##### (Z)-4-((2-((6-methylbenzofuran-3(2H)-ylidene)amino)thiazol-4-yl)amino)benzenesulfonamide (5c)

Follow up the general method above, compound 3 (0.54 g, 2 mmol), two drops of glacial acetic acid and 6-methylbenzofuran-3(2H)-one (0.30 gm, 2 mmol). The final analogue obtained as orange powder (65%). mp = 202–205 °C;  $^1H$  NMR (DMSO- $d_6$ )  $\delta$ : 7.78-7.69 (m, 4H, Aromatic-H), 7.49 (broad s, 1H, N-H), 7.32-7.25 (m, 2H, Ar-H) 7.09 (s, 2H,  $NH_2SO_2$ ), 6.89 (d, 1H, Ar-H), 5.78 (s, 1H, s, thiazole CH), 4.92 (s, 2H, cyclic O-CH<sub>2</sub>), 3.21 (s, 3H, CH<sub>3</sub>).  $^{13}C$  NMR (DMSO- $d_6$ ,  $\delta$ ):  $\delta$  197.89, 158.54, 156.98, 103.54, 138.89-73.65 (13 Ar-C), 26.98, TLC:  $R_f$ 0.79<sup>a</sup>.

##### (Z)-4-((2-((6-methoxybenzofuran-3(2H)-ylidene)amino)thiazol-4yl)amino)benzenesulfonamide (5d)

Follow up the general method above, compound 3 (0.54 g, 2 mmol), two drops of glacial acetic acid and 6-

methoxybenzofuran-3(2H)-one (0.33 gm, 2 mmol). The final analogue obtained as orange powder (65%). mp = 207–209 °C; <sup>1</sup>H NMR (DMSO-*d*<sub>6</sub>) δ: 7.67-7.52 (m, 4H, Aromatic-H), 7.49 (broad s, 1H, N-H), 7.15-7.02 (m, 2H, Ar-H) 6.89 (s, 2H, NH<sub>2</sub>SO<sub>2</sub>), 6.64 (d, 2H, Aromatic-H), 5.86 (s, 1H, s, thiazole CH), 4.68 (s, 2H, cyclic O-CH<sub>2</sub>), 3.45 (s, 3H, OCH<sub>3</sub>). <sup>13</sup>C NMR (DMSO-*d*<sub>6</sub>, δ): δ 197.98, 158.11, 156.56, 103.43, 138.86-74.56 (13 Ar-C), 32.87, TLC: *R*<sub>f</sub>0.77<sup>a</sup>.

#### Docking study

Docking study were applied by using Schrodinger Maestro software release (version 2021-1). Both protein and ligand structures were prepared prior to simulation. Ligand preparation involved protonation of the 3D structures, assignment of partial charges, and energy minimisation to obtain stable conformations. Protein Data Bank was used to obtain the CA IX protein (PDB ID: 4Z0Q). Before docking, the protein was prepared by removing water molecules and any unnecessary components so that the ligand could interact properly with it. Missing hydrogen atoms were added, incomplete bonds were fixed, and the protein structure was optimised for docking. Using Schrödinger Maestro software, the active site of CA IX was identified, which helped determine the key amino acid residues involved in ligand binding.

Docking simulations were then used to study how the ligands might interact with and bind to the CA protein. The results showed that, in its deprotonated form, the sulfonamide nitrogen carries a negative charge that allows it to bind to the catalytic zinc ion (Zn<sup>2+</sup>). This interaction is further supported by hydrogen bonding, particularly with the Thr199 residue. The engaged performance of the synthesised compounds was assessed using docking scores (S-scores) and root mean square deviation (RMSD) values. The S-score reflects the predicted strength of binding between the ligand and the protein, with lower values indicating stronger interactions, while RMSD indicates how closely the predicted binding pose matches the reference structure.

#### Cytotoxic study

The antiproliferative activity of the synthesised dihydrobenzofuran compounds (5a–5d) was tested using the MTT assay. Three cell lines were used: MCF-7 and HCT116 to evaluate anticancer activity, and MCF10A (normal breast cells) to assess effects on non-cancerous cells. MCF-7 and HCT116 were in RPMI medium, while MCF10A were cultured in DMEM medium. All media were supplemented as research provide with fetal bovine serum (FBS, 10%) and using antibiotic streptomycin in concentration 100 µg/mL and penicillin with 100 U/mL. Incubated the cells were obtained at 37°C in 5% CO<sub>2</sub> of humidified atmosphere. For routine sub culturing, different solution of trypsin/EDTA (Gibco) and phosphate-buffered saline (PBS) were used.

For the assay, cells were seeded into 96 cells/ well plates at a density of 1.4 × 10<sup>4</sup> cells per well in 200 µL of fresh medium and to allow cell attachment it was incubated to overnight. 24 h later, the cells treated through using different concentrations of the synthesised compounds and positive controls (doxorubicin). Following treatment, the culture medium was removed, and 200 µL of MTT was added to each

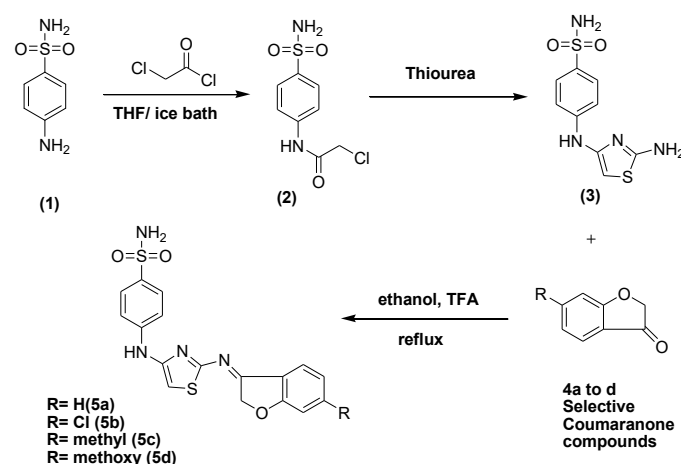
well. Plates were then incubated for 4 hours at 37°C to allow formation of formazan crystals. Then, 100 µL of dimethyl sulfoxide (DMSO) was added to help in dissolve the crystals, and the plates were gently shaken at 37°C until they were completely dissolved. To measure the absorbance at 570 nm an ELISA plate reader (Model Wave XS2, BioTek) was used, and the IC<sub>50</sub> values were calculated based on these measurements.

### III. RESULTS AND DISCUSSION

#### General chemistry

The synthesis of the dihydrobenzofuran compounds (5a–5d) is shown in Scheme 1. The process started with sulphanilamide (1), which was reacted with chloroacetyl chloride in tetrahydrofuran (THF) using K<sub>2</sub>CO<sub>3</sub>. This reaction produced a sulfanilamide chloroacetyl intermediate (2). This intermediate subsequently underwent cyclisation with thiourea to afford the thiazole-containing compound (3). (22)

The final analogues (5a–5c) were generated by coupling thiazole intermediate 3 with suitably substituted aromatic dihydrobenzofuran moieties. Substituents at the 4-position—including hydrogen, chlorine, methyl, and methoxy groups—were selected based on prior evidence suggesting enhanced binding interactions and favourable orientation within the enzyme active site. The desired products were obtained in high purity (>95%) following recrystallization, therefore purification by column chromatography was not applied. Structural confirmation of compounds 5a–5d was achieved using both <sup>1</sup>H and <sup>13</sup>C nuclear magnetic resonance (NMR) spectroscopy.



Scheme 1: Synthetic route of compounds 2, 3 and dihydrobenzofuran derivatives 5a to 5d.

#### Molecular docking findings

The docking scores of dihydrobenzofuran derivatives 5a to 5d and AZM on CA isoforms (CA IX) are explained in Table 1, and the two-dimensional (2D) interactions of all compounds 5a-5d and AZM with active site of CA IX are in Figures 1. The docking results revealed differences in binding affinity among the synthesised compounds, with 5a, 5b and 5d demonstrating particularly strong interactions within the active site of carbonic anhydrase IX. As shown in table 1, the lower

S-scores and RMSD values for derivatives 5a, 5b and 5d indicate a stronger predicted binding affinity.

TABLE 1. Docking study results of synthesised dihydrobenzofuran derivatives 5a to 5d.

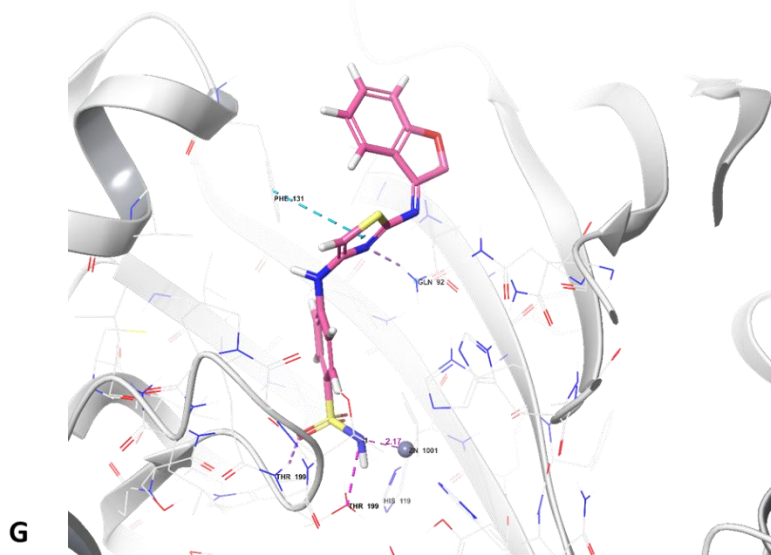
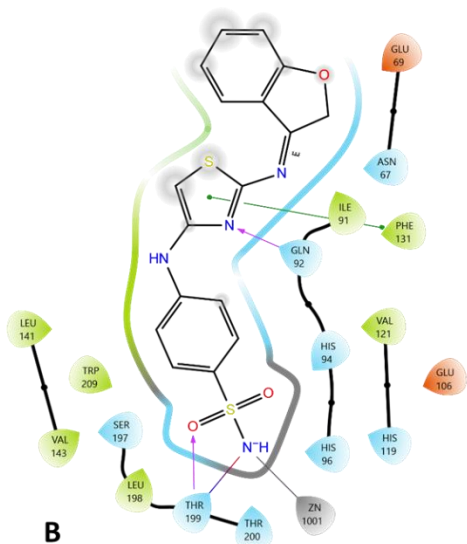
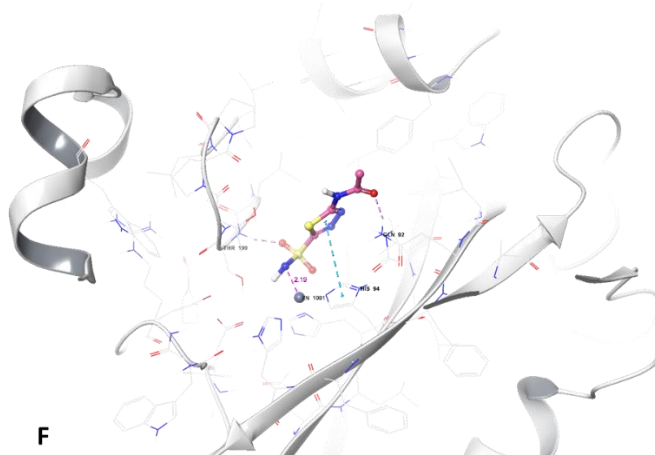
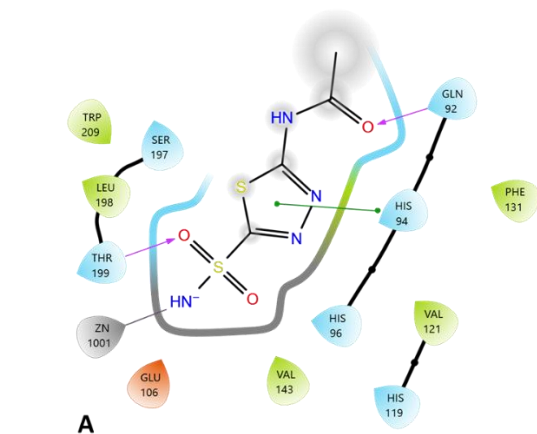
Analogue	S scores	RMSD	Interacting residues
Acetazolamide	-5.573	2.095	Zn1001, Thr 199, His 94, Gln 92
5a	-6.852	1.385	Zn1001, Thr 199, Phe 131, Gln 92
5b	-7.346	2.045	Zn1001, Thr 199, His 64, Trp 5
5c	-6.694	1.698	Zn1001, Thr 199
5d	-6.958	1.995	Zn1001, Thr 199, Phe 131, Trp 5

Docking studies indicated that the synthesised compounds particularly 5b and 5d exhibit favourable interactions within the active site of the target protein. The sulfonamide group seems to be important for binding to the catalytic site, while the thiazole ring likely helps the molecule fit properly into the binding pocket and keeps the imine group in the right position. Compounds 5b and 5d exhibited a good interactions with the receptor binding site similar to the AZM. Table 1 showed that compound 5b have low value of S-score, which suggest that this compound could be have strong binding affinity and good

interaction with the protein. On the other hand, 5a had a low RMSD value, meaning its predicted binding position is very close to the ideal binding conformation. Acetazolamide, by comparison, exhibited higher S-score and RMSD values, reflecting weaker predicted binding. Overall, these findings suggest that the newly synthesised compounds have potential as carbonic anhydrase IX inhibitors, supporting their further investigation as candidates for anticancer drug development.

*Evaluate of cytotoxicity*

The cytotoxic potential of the synthesised dihydrobenzofuran derivatives (5a–5d) was assessed in comparison with doxorubicin as a reference standard. In vitro antiproliferative activity was evaluated against breast (MCF-7) and colon (HCT116) cancer cell lines, while cytotoxicity toward non-tumorigenic breast epithelial cells (MCF10A) was also examined to estimate selectivity. The MCF-7 was selected based on its well-established relation in reflecting breast cancer drug sensitivity, whereas HCT116 cells, known for their aggressive and highly tumorigenic nature, are widely used in anticancer drug screening. IC<sub>50</sub> values were determined for all compounds, with doxorubicin serving as a positive control (Table 2).



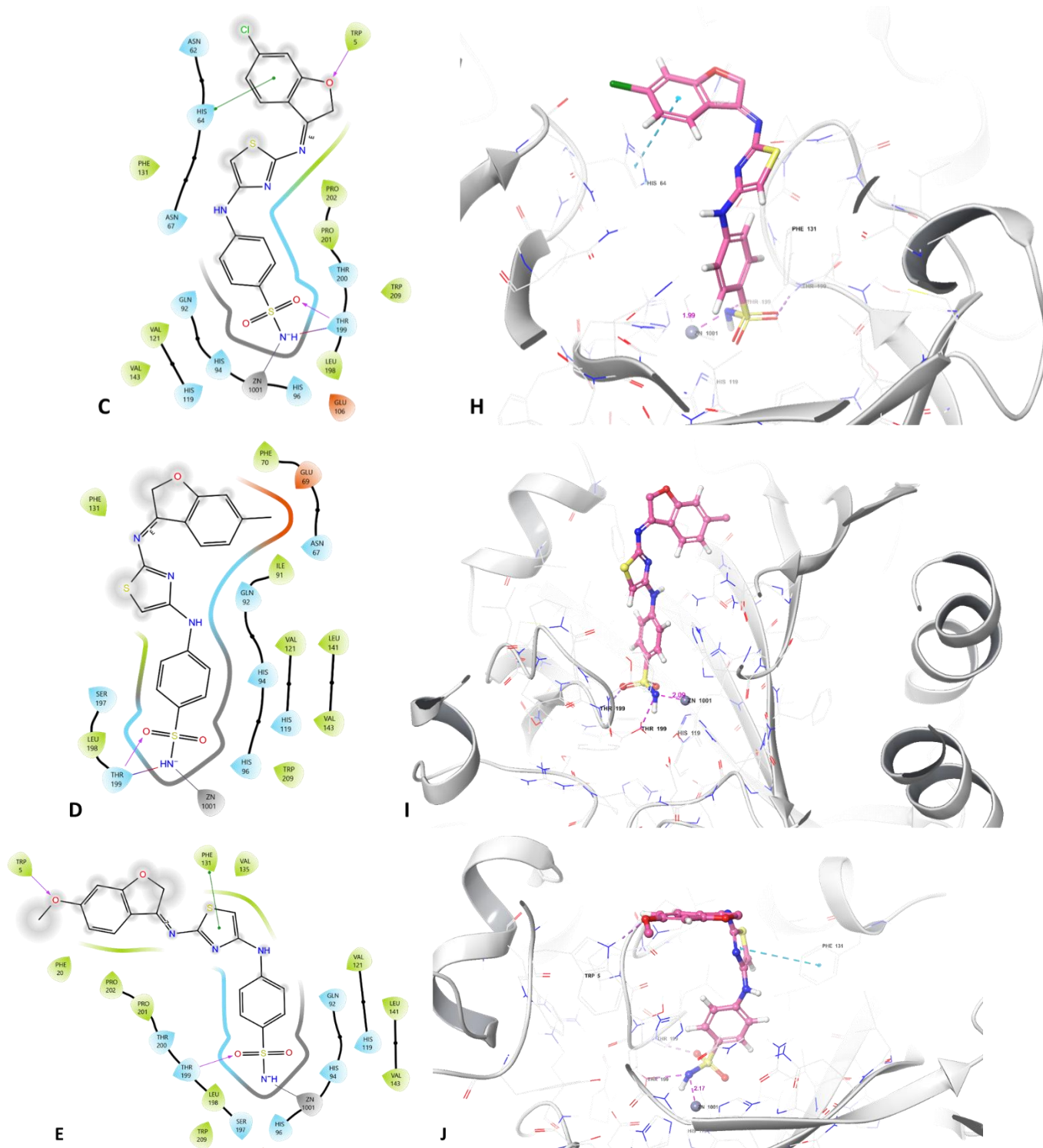


Figure 1: Predicted binding docked pose of dihydrobenzofuran derivatives 5a to 5d within the active site of CA IX (CODE: 4Z0Q): (A, B, C, D, E) representation of interacting residues which could be involved in interact with CAIX for analogues AZM and dihydrobenzofuran derivatives 5a to 5d respectively; (F, G, H, I, J) dihydrobenzofuran derivatives 5a to 5d binding mode; (Schrodinger Maestro software release 2021-1).

As expected, doxorubicin demonstrated strong cytotoxic potency versus both MCF- 7 and HCT-116 cell lines ( $IC_{50} = 1.10 \pm 0.02 \mu M$  and  $1.07 \pm 0.05 \mu M$ , respectively). In contrast, the test compounds exhibited variable levels of activity and selectivity. Compounds with  $IC_{50}$  values below  $10 \mu M$  were considered biologically active. Among them, derivative 5b,

bearing a chlorine atom at C3-position on the dihydrobenzofuran ring, showed moderate activity versus both MCF- 7 and HCT-116 cells ( $IC_{50} = 8.68 \pm 0.87 \mu M$  and  $7.24 \pm 0.81 \mu M$ , respectively). Compound 5d, containing a methoxy substituent, also demonstrated moderate cytotoxicity against MCF-7 cells ( $IC_{50} = 9.24 \pm 0.90 \mu M$ ) but was less

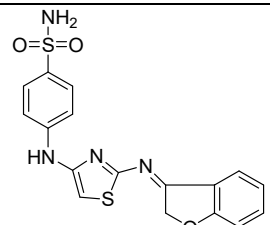
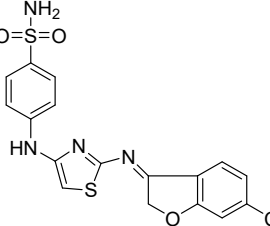
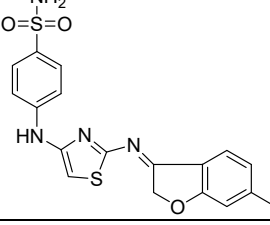
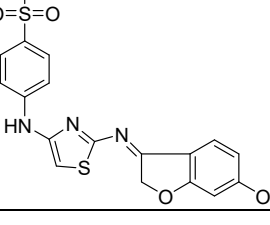
effective against HCT116 cells ( $IC_{50} = 15.33 \pm 1.21 \mu M$ ). In contrast, compounds 5a and 5c, substituted with hydrogen or methyl groups at the C3-position, showed comparatively lower activity against both cancer cell lines, the MCF-7 ( $IC_{50} = 14.49 \pm 1.09$  and  $13.01 \pm 1.51 \mu M$ , respectively) and HCT116 cell line ( $IC_{50} = 15.37 \pm 1.12$  and  $11.29 \pm 1.03 \mu M$ , respectively).

To assess safety and selectivity, the compounds were also tested on normal MCF10A cells. Doxorubicin exhibited high level of toxicity toward normal cells ( $IC_{50} = 1.40 \pm 0.02 \mu M$ ).

In comparison, compound 5d was less toxic to normal cells ( $IC_{50} = 16.21 \pm 1.13 \mu M$ ), and compound 5b showed even lower toxicity ( $IC_{50} = 17.01 \pm 1.21 \mu M$ ), suggesting better selectivity.

Overall, these results suggest that the dihydrobenzofuran compounds 5b and 5d have a valuable anticancer strength and selectivity and its appears promising compounds having good anticancer activity with lower toxicity to normal cells.

TABLE 2: The results of Cytotoxicity evaluation for the dihydrobenzofuran derivatives (5a-d).

Compound number	Structure	IC <sub>50</sub> values ( $\mu M \pm SD$ )		
		MCF-7	HCT116	HCF10a
Doxorubicin	---	1.10 $\pm$ 0.02	1.07 $\pm$ 0.05	1.40 $\pm$ 0.02
Compound 5a		14.49 $\pm$ 1.09	15.37 $\pm$ 1.12	16.01 $\pm$ 1.12
Compound 5b		8.68 $\pm$ 0.87	7.24 $\pm$ 0.81	17.01 $\pm$ 1.21
Compound 5c		13.01 $\pm$ 1.51	11.29 $\pm$ 1.03	12.31 $\pm$ 1.03
Compound 5d		9.24 $\pm$ 0.90	15.33 $\pm$ 1.21	16.21 $\pm$ 1.13

#### IV. CONCLUSION

Successful synthesis and characterisation of a series of dihydrobenzofuran compounds (5a–5d) has been explored in this study. The synthesised compounds started from sulfanilamide and dihydrobenzofuran as key starting materials. The structures of final compounds were confirmed by using <sup>1</sup>H-NMR and <sup>13</sup>C-NMR. Furthermore, the MTT assay by using three cell lines (MCF-7, HCT-116 and MCF10A) was applied to evaluate the biological activity of these compounds. Both compounds 5b which contain chlorine (Cl) and 5d, which

contain chlorine methoxy moiety at the C3 of the dihydrobenzofuran, showed higher cytotoxic activity. Overall, these results highly recommended that compounds 5b and 5d could be promising candidates for further development as potential anticancer agents.

#### REFERENCES

- [1]. Sun, K. X., Liang, X., Zhu, Q., Wu, H. L., Zhang, G. Y., Yao, Y. F., Li, X., Zheng, R. S., Zuo, J., & Wei, W. Q. (2025). Global patterns and trends in cancer-related premature death and their impact on life expectancy across 185 countries: a population-based analysis. *Military*

- Medical Research*, 12(1), 56. <https://doi.org/10.1186/s40779-025-00645-9>.
- [2]. Iburg, K. M., Mikkelsen, L., Adair, T., & Lopez, A. D. (2020). Are cause of death data fit for purpose? evidence from 20 countries at different levels of socio-economic development. *PLoS one*, 15(8), e0237539. <https://doi.org/10.1371/journal.pone.0237539>.
- [3]. Huang, Q., Li, Y., Huang, Y., Wu, J., Bao, W., Xue, C., Li, X., Dong, S., Dong, Z., & Hu, S. (2025). Advances in molecular pathology and therapy of non-small cell lung cancer. *Signal transduction and targeted therapy*, 10(1), 186. <https://doi.org/10.1038/s41392-025-02243-6>.
- [4]. Mbogge, M. Y., Mahon, B. P., McKenna, R., & Frost, S. C. (2018). Carbonic Anhydrases: Role in pH Control and Cancer. *Metabolites*, 8(1), 19. <https://doi.org/10.3390/metabo8010019>.
- [5]. Chen, A. Y., Adamek, R. N., Dick, B. L., Credille, C. V., Morrison, C. N., & Cohen, S. M. (2019). Targeting Metalloenzymes for Therapeutic Intervention. *Chemical reviews*, 119(2), 1323–1455. <https://doi.org/10.1021/acs.chemrev.8b00201>.
- [6]. Le Goff, C., Ganot, P., Zoccola, D., Caminiti-Segonds, N., Allemand, D., & Tambutti, S. (2016). Carbonic Anhydrases in Cnidarians: Novel Perspectives from the Octocorallian *Corallium rubrum*. *PLoS one*, 11(8), e0160368. <https://doi.org/10.1371/journal.pone.0160368>.
- [7]. Telkoparan-Akillilar, P., Chichiarelli, S., Tucci, P., & Saso, L. (2025). Integration of MicroRNAs with nanomedicine: tumor targeting and therapeutic approaches. *Frontiers in cell and developmental biology*, 13, 1569101. <https://doi.org/10.3389/fcell.2025.1569101>.
- [8]. Reda El Sayed, S., Cristante, J., Guyon, L., Denis, J., Chabre, O., & Cherradi, N. (2021). MicroRNA Therapeutics in Cancer: Current Advances and Challenges. *Cancers*, 13(11), 2680. <https://doi.org/10.3390/cancers13112680>.
- [9]. Li, S., Gong, J., Kang, B., Wang, Z., Ma, Y., Xia, X., & Yan, H. (2026). Targeting Glycolytic Metabolism in Cancer Therapy: Current Approaches and Future Perspectives. *Cells*, 15(4), 362. <https://doi.org/10.3390/cells15040362>.
- [10]. Supuran C. T. (2016). How many carbonic anhydrase inhibition mechanisms exist?. *Journal of enzyme inhibition and medicinal chemistry*, 31(3), 345–360. <https://doi.org/10.3109/14756366.2015.1122001>.
- [11]. Lomelino, C. L., Supuran, C. T., & McKenna, R. (2016). Non-Classical Inhibition of Carbonic Anhydrase. *International journal of molecular sciences*, 17(7), 1150. <https://doi.org/10.3390/ijms17071150>.
- [12]. Supuran C. T. (2025). Multi- and polypharmacology of carbonic anhydrase inhibitors. *Pharmacological reviews*, 77(1), 100004. <https://doi.org/10.1124/pharmrev.124.001125>.
- [13]. Petrou, A., Fesatidou, M., & Geronikaki, A. (2021). Thiazole Ring-A Biologically Active Scaffold. *Molecules (Basel, Switzerland)*, 26(11), 3166. <https://doi.org/10.3390/molecules26113166>.
- [14]. Ayati, A., Emami, S., Moghimi, S., & Foroumadi, A. (2019). Thiazole in the targeted anticancer drug discovery. *Future medicinal chemistry*, 11(15), 1929–1952. <https://doi.org/10.4155/fmc-2018-0416>.
- [15]. Khamitova, A., Berillo, D., Lozynskiy, A., Konechniy, Y., Mural, D., Georgiyants, V., & Lesyk, R. (2024). Thiadiazole and Thiazole Derivatives as Potential Antimicrobial Agents. *Mini reviews in medicinal chemistry*, 24(5), 531–545. <https://doi.org/10.2174/1389557523666230713115947>.
- [16]. Sharma, P. C., Bansal, K. K., Sharma, A., Sharma, D., & Deep, A. (2020). Thiazole-containing compounds as therapeutic targets for cancer therapy. *European journal of medicinal chemistry*, 188, 112016. <https://doi.org/10.1016/j.ejmech.2019.112016>.
- [17]. Mohamed, G. G., & Sharaby, C. M. (2007). Metal complexes of Schiff base derived from sulphametrole and o-vanilin. Synthesis, spectral, thermal characterization and biological activity. *Spectrochimica acta. Part A, Molecular and biomolecular spectroscopy*, 66(4-5), 949–958. <https://doi.org/10.1016/j.saa.2006.04.033>.
- [18]. Ebrahimi, H. P., Hadi, J. S., Almayah, A. A., Bolandnazar, Z., Swadi, A. G., & Ebrahimi, A. (2016). Metal-based biologically active azoles and  $\beta$ -lactams derived from sulfa drugs. *Bioorganic & medicinal chemistry*, 24(5), 1121–1131. <https://doi.org/10.1016/j.bmc.2016.01.041>.
- [19]. Anacona, J. R., Noriega, N., & Camus, J. (2015). Synthesis, characterization and antibacterial activity of a tridentate Schiff base derived from cephalothin and sulfadiazine, and its transition metal complexes. *Spectrochimica acta. Part A, Molecular and biomolecular spectroscopy*, 137, 16–22. <https://doi.org/10.1016/j.saa.2014.07.091>.
- [20]. Macias, B., Villa, M. V., Sanz, F., Borrás, J., González-Alvarez, M., & Alzuet, G. (2005). Cu(II) complexes with a sulfonamide derived from benzoguanamine. Oxidative cleavage of DNA in the presence of H<sub>2</sub>O<sub>2</sub> and ascorbate. *Journal of inorganic biochemistry*, 99(7), 1441–1448. <https://doi.org/10.1016/j.jinorgbio.2005.04.001>.
- [21]. Sharaby C. M. (2007). Synthesis, spectroscopic, thermal and antimicrobial studies of some novel metal complexes of Schiff base derived from [N1-(4-methoxy-1,2,5-thiadiazol-3-yl)sulfanilamide] and 2-thiophene carboxaldehyde. *Spectrochimica acta. Part A, Molecular and biomolecular spectroscopy*, 66(4-5), 1271–1278. <https://doi.org/10.1016/j.saa.2006.05.030>.
- [22]. Sarathi Addy, P., Saha, B., Pradeep Singh, N. D., Das, A. K., Bush, J. T., Lejeune, C., Schofield, C. J., & Basak, A. (2013). 1,3,5-Trisubstituted benzenes as fluorescent photoaffinity probes for human carbonic anhydrase II capture. *Chemical communications (Cambridge, England)*, 49(19), 1930–1932. <https://doi.org/10.1039/c3cc38251f>.
- [23]. Abbas, H. S., Abd El-Karim, S. S., & Abdelwahed, N. A. M. (2017). Synthesis and biological evolution of sulphonamide derivatives as antimicrobial agents. *Acta poloniae pharmaceutica*, 74(3), 849–860. <https://doi.org/10.1078/j.aps.2017.01.0678>.